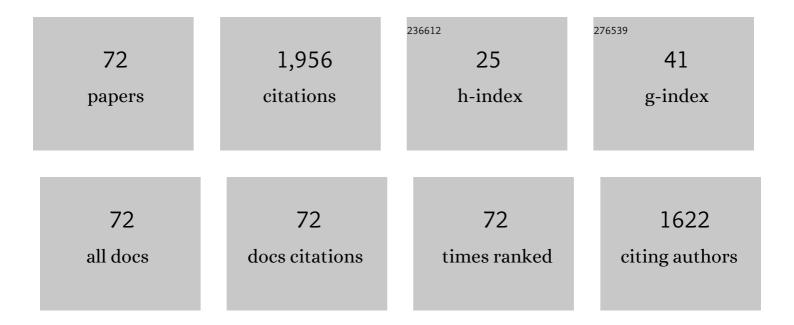
RadomÃ-r \ddot{A} Cerstv $\tilde{A}^{1/2}$

List of Publications by Year in descending order

Source: https://exaly.com/author-pdf/1680657/publications.pdf Version: 2024-02-01



#	Article	IF	CITATIONS
1	Structure and properties of hard and superhard Zr–Cu–N nanocomposite coatings. Materials Science & Engineering A: Structural Materials: Properties, Microstructure and Processing, 2000, 289, 189-197.	2.6	139
2	Thermal stability of alumina thin films containing Î ³ -Al2O3 phase prepared by reactive magnetron sputtering. Applied Surface Science, 2010, 257, 1058-1062.	3.1	115
3	Tribological and mechanical properties of nanocrystalline-TiC/a-C nanocomposite thin films. Journal of Vacuum Science and Technology A: Vacuum, Surfaces and Films, 2010, 28, 244-249.	0.9	114
4	Structure–property relations of arc-evaporated Al–Cr–Si–N coatings. Surface and Coatings Technology, 2008, 202, 3555-3562.	2.2	78
5	Role of energy in low-temperature high-rate formation of hydrophilic TiO2 thin films using pulsed magnetron sputtering. Journal of Vacuum Science and Technology A: Vacuum, Surfaces and Films, 2007, 25, 666-674.	0.9	73
6	Amorphous Zr-Cu thin-film alloys with metallic glass behavior. Journal of Alloys and Compounds, 2017, 696, 1298-1306.	2.8	73
7	Process stabilization and a significant enhancement of the deposition rate in reactive high-power impulse magnetron sputtering of ZrO2 and Ta2O5 films. Surface and Coatings Technology, 2013, 236, 550-556.	2.2	72
8	Properties of magnetron sputtered Al–Si–N thin films with a low and high Si content. Surface and Coatings Technology, 2008, 202, 3485-3493.	2.2	56
9	Nanostructure of photocatalytic TiO2 films sputtered at temperatures below 200°C. Applied Surface Science, 2008, 254, 3793-3800.	3.1	55
10	High-rate reactive high-power impulse magnetron sputtering of hard and optically transparent HfO 2 films. Surface and Coatings Technology, 2016, 290, 58-64.	2.2	49
11	Transparent Zr–Al–O oxide coatings with enhanced resistance to cracking. Surface and Coatings Technology, 2012, 206, 2105-2109.	2.2	48
12	Significant improvement of the performance of ZrO2/V1-W O2/ZrO2 thermochromic coatings by utilizing a second-order interference. Solar Energy Materials and Solar Cells, 2019, 191, 365-371.	3.0	46
13	Effect of the gas mixture composition on high-temperature behavior of magnetron sputtered Si–B–C–N coatings. Surface and Coatings Technology, 2008, 203, 466-469.	2.2	42
14	Thermal stability of magnetron sputtered Si–B–C–N materials at temperatures up to 1700°C. Thin Solid Films, 2010, 519, 306-311.	0.8	41
15	Two-phase single layer Al-O-N nanocomposite films with enhanced resistance to cracking. Surface and Coatings Technology, 2012, 206, 4230-4234.	2.2	39
16	Controlled reactive HiPIMS—effective technique for low-temperature (300 °C) synthesis of VO ₂ films with semiconductor-to-metal transition. Journal Physics D: Applied Physics, 2017, 50, 38LT01.	1.3	38
17	Properties of nanocrystalline Al–Cu–O films reactively sputtered by DC pulse dual magnetron. Applied Surface Science, 2011, 258, 1762-1767.	3.1	36
18	Hard and superhard nanocomposite Al–Cu–N films prepared by magnetron sputtering. Surface and Coatings Technology, 2001, 142-144, 603-609.	2.2	33

RADOMÃR ÄŒERSTVý

#	Article	IF	CITATIONS
19	The effect of addition of Al in ZrO2 thin film on its resistance to cracking. Surface and Coatings Technology, 2012, 207, 355-360.	2.2	32
20	Flexible hydrophobic ZrN nitride films. Vacuum, 2016, 131, 34-38.	1.6	30
21	High-rate reactive high-power impulse magnetron sputtering of Ta–O–N films with tunable composition and properties. Thin Solid Films, 2014, 566, 70-77.	0.8	29
22	Thickness dependent wetting properties and surface free energy of HfO2 thin films. Applied Physics Letters, 2016, 108, .	1.5	28
23	Superior high-temperature oxidation resistance of magnetron sputtered Hf–B–Si–C–N film. Ceramics International, 2016, 42, 4853-4859.	2.3	28
24	Magnetron sputtered Si–B–C–N films with high oxidation resistance and thermal stability in air at temperatures above 1500 °C. Journal of Vacuum Science and Technology A: Vacuum, Surfaces and Films, 2008, 26, 1101-1108.	0.9	27
25	Effect of positive pulse voltage in bipolar reactive HiPIMS on crystal structure, microstructure and mechanical properties of CrN films. Surface and Coatings Technology, 2020, 393, 125773.	2.2	27
26	Properties of thermochromic VO2 films prepared by HiPIMS onto unbiased amorphous glass substrates at a low temperature of 300â€ ⁻ °C. Thin Solid Films, 2018, 660, 463-470.	0.8	26
27	Antibacterial Cr–Cu–O films prepared by reactive magnetron sputtering. Applied Surface Science, 2013, 276, 660-666.	3.1	25
28	Evolution of microstructure and macrostress in sputtered hard Ti(Al,V)N films with increasing energy delivered during their growth by bombarding ions. Journal of Vacuum Science and Technology A: Vacuum, Surfaces and Films, 2017, 35, .	0.9	25
29	Hard nanocrystalline Zr–B–C–N films with high electrical conductivity prepared by pulsed magnetron sputtering. Surface and Coatings Technology, 2013, 215, 186-191.	2.2	23
30	Effect of energy on structure, microstructure and mechanical properties of hard Ti(Al,V)Nx films prepared by magnetron sputtering. Surface and Coatings Technology, 2017, 332, 190-197.	2.2	23
31	Pulsed reactive magnetron sputtering of high-temperature Si–B–C–N films with high optical transparency. Surface and Coatings Technology, 2013, 226, 34-39.	2.2	22
32	Thermal effects of laser marking on microstructure and corrosion properties of stainless steel. Applied Optics, 2016, 55, D35.	2.1	22
33	Structure and properties of Hf-O-N films prepared by high-rate reactive HiPIMS with smoothly controlled composition. Ceramics International, 2017, 43, 5661-5667.	2.3	22
34	Two-functional DC sputtered Cu-containing TiO2 thin films. Journal of Photochemistry and Photobiology A: Chemistry, 2010, 209, 158-162.	2.0	20
35	Hard multifunctional Hf–B–Si–C films prepared by pulsed magnetron sputtering. Surface and Coatings Technology, 2014, 257, 301-307.	2.2	20
36	Tribological properties and oxidation resistance of tungsten and tungsten nitride films at temperatures up to 500†°C. Tribology International, 2019, 132, 211-220.	3.0	20

RADOMÃR ÄŒERSTVý

#	Article	IF	CITATIONS
37	Two-Functional Direct Current Sputtered Silver-Containing Titanium Dioxide Thin Films. Nanoscale Research Letters, 2009, 4, 313-320.	3.1	19
38	Effect of energy on the formation of flexible hard Al-Si-N films prepared by magnetron sputtering. Vacuum, 2016, 133, 43-45.	1.6	19
39	Flexible antibacterial Al–Cu–N films. Surface and Coatings Technology, 2015, 264, 114-120.	2.2	18
40	Formation of crystalline Al–Ti–O thin films and their properties. Surface and Coatings Technology, 2008, 202, 6064-6069.	2.2	17
41	Flexible antibacterial Zr-Cu-N thin films resistant to cracking. Journal of Vacuum Science and Technology A: Vacuum, Surfaces and Films, 2016, 34, .	0.9	17
42	Coefficient of friction and wear of sputtered a-C thin coatings containing Mo. Surface and Coatings Technology, 2010, 205, 1486-1490.	2.2	16
43	l²- (Me1, Me2) and MeNx films deposited by magnetron sputtering: Novel heterostructural alloy and compound films. Surface and Coatings Technology, 2018, 337, 75-81.	2.2	16
44	Protection of brittle film against cracking. Applied Surface Science, 2016, 370, 306-311.	3.1	15
45	Microwave plasma nitriding of a low-alloy steel. Journal of Vacuum Science and Technology A: Vacuum, Surfaces and Films, 2000, 18, 2715-2721.	0.9	14
46	Thermally activated transformations in metastable alumina coatings prepared by magnetron sputtering. Surface and Coatings Technology, 2014, 240, 7-13.	2.2	14
47	Dependence of characteristics of MSiBCN (M = Ti, Zr, Hf) on the choice of metal element: Experimental and ab-initio study. Thin Solid Films, 2016, 616, 359-365.	0.8	14
48	Protective Zr-containing SiO2 coatings resistant to thermal cycling in air up to 1400°C. Surface and Coatings Technology, 2009, 203, 1502-1507.	2.2	13
49	Pulsed Magnetron Sputtering of Strongly Thermochromic VO2-Based Coatings with a Transition Temperature of 22 ŰC onto Ultrathin Flexible Glass. Coatings, 2020, 10, 1258.	1.2	11
50	Control of structure in magnetron sputtered thin films. Surface and Coatings Technology, 2001, 142-144, 201-205.	2.2	10
51	Mechanical and tribological properties of sputtered Mo–O–N coatings. Surface and Coatings Technology, 2013, 215, 386-392.	2.2	10
52	Dependence of structure and properties of hard nanocrystalline conductive films MBCN (M = Ti, Zr,) Tj ETQq0 0	Ͻ rgBT /Ον	erlock 10 Tf
53	Effect of energy on macrostress in Ti(Al,V)N films prepared by magnetron sputtering. Vacuum, 2018, 158, 52-59.	1.6	10

54Impact of Al or Si addition on properties and oxidation resistance of magnetron sputtered2.81054Zr–Hf–Al/Si–Cu metallic glasses. Journal of Alloys and Compounds, 2019, 772, 409-417.2.810

RADOMÃR ÄŒERSTVý

#	Article	IF	CITATIONS
55	Effect of annealing on structure and properties of Ta–O–N films prepared by high power impulse magnetron sputtering. Ceramics International, 2019, 45, 9454-9461.	2.3	10
56	Transfer of the sputter technique for deposition of strongly thermochromic VO2-based coatings on ultrathin flexible glass to large-scale roll-to-roll device. Surface and Coatings Technology, 2022, 442, 128273.	2.2	10
57	Physical and mechanical properties of Ti/Al multilayer heat releasing coatings. International Journal of Nanomanufacturing, 2015, 11, 78.	0.3	9
58	(Zr,Ti,O) alloy films with enhanced hardness and resistance to cracking prepared by magnetron sputtering. Surface and Coatings Technology, 2017, 322, 86-91.	2.2	9
59	Flexible hard (Zr, Si) alloy films prepared by magnetron sputtering. Thin Solid Films, 2019, 688, 137216.	0.8	9
60	Dependence of the ZrO2 growth on the crystal orientation: growth simulations and magnetron sputtering. Applied Surface Science, 2022, 572, 151422.	3.1	9
61	Tuning properties and behavior of magnetron sputtered Zr-Hf-Cu metallic glasses. Journal of Alloys and Compounds, 2018, 739, 848-855.	2.8	8
62	Reactive high-power impulse magnetron sputtering of ZrO2 films with gradient ZrOx interlayers on pretreated steel substrates. Journal of Vacuum Science and Technology A: Vacuum, Surfaces and Films, 2017, 35, 031503.	0.9	7
63	Thermal stability of structure, microstructure and enhanced properties of Zr–Ta–O films with a low and high Ta content. Surface and Coatings Technology, 2018, 335, 95-103.	2.2	5
64	Tunable composition and properties of Al-O-N films prepared by reactive deep oscillation magnetron sputtering. Surface and Coatings Technology, 2020, 392, 125716.	2.2	5
65	Extraordinary high-temperature behavior of electrically conductive Hf7B23Si22C6N40 ceramic film. Surface and Coatings Technology, 2020, 391, 125686.	2.2	5
66	Oxidation of Sputtered Cu, Zr, ZrCu, ZrO2, and Zr-Cu-O Films during Thermal Annealing in Flowing Air. Plasma Processes and Polymers, 2007, 4, S536-S540.	1.6	4
67	Thermal co-decomposition of silver acetylacetonate and tin(II) hexafluoroacetylacetonate: Formation of carbonaceous Ag/AgxSn(x=4 and 6.7)/SnO2 composites. Thermochimica Acta, 2013, 566, 92-99.	1.2	4
68	Hard TiN2 dinitride films prepared by magnetron sputtering. Journal of Vacuum Science and Technology A: Vacuum, Surfaces and Films, 2018, 36, .	0.9	4
69	Thermal stability and transformation phenomena in magnetron sputtered Al–Cu–O films. Ceramics International, 2015, 41, 6020-6029.	2.3	3
70	Coating of overstoichiometric transition metal nitrides (TMN _x (x > 1)) by magnetron sputtering. Japanese Journal of Applied Physics, 2019, 58, SAAD10.	0.8	3
71	Effect of Nitrogen Content on the Microstructure and Hardness of Hard Zr–B–C–N Films. Microscopy and Microanalysis, 2014, 20, 1892-1893.	0.2	2
72	Mechanical and tribological properties of Sn-Cu-O films prepared by reactive magnetron sputtering. Journal of Vacuum Science and Technology A: Vacuum, Surfaces and Films, 2014, 32, 021504.	0.9	1